Sintering temperature dependent multiferroic properties of Mn substituted $BiFeO_3$

U. K. Wadane[1], V. K. Barote[2], S. S. More[3], S. K. Gurav[4], S. B. Shelke[4]*, A. R. Shitre[3]

[1]Department of Physics, Terna Engineering College, Osmanabad (M.S.) India
[2]Department of Physics, Sant Dnyaneshwar College, Soegaon, Aurangabad (M.S.) India
[3]Physics Department, Y. C. College, Tuljapur, Dist. Osmanabad (M.S.) India
[4]Physics Department, S. M. P. College, Murum, Tq. Omerga, Dist. Osmanabad (M.S.) India
[*] Corresponding Author: drsbshellke@gmail.com

Abstract

Mn substituted $BiFeO_3$ with a chemical formula $BiMn_{0.2}Fe_{0.8}O_3$ is synthesized by the sol-gel auto-combustion method. Crystal structure phase of all the prepared samples were investigated by X-ray diffraction (XRD) pattern. Rhombohedral phase (space group $R3_c$) in combination with some other phases were observed in all the samples. Lattice constants decreased from a = 5.582 Å, c = 13.724 Å to a = 5.571 Å, c = 13.718 Å with the increase in sintering temperature. Crystallite size obtained from XRD pattern increased from 25 to 48 nm with the increase in sintering temperature. Variation in polarization with applied electric field was studied to study the ferroelectric behaviour of the prepared samples. Magnetic properties were investigated using magnetization versus applied magnetic field hysteresis loops. Value of dielectric constant was obtained by measuring the dielectric properties using LCR-Q meter. It has been observed that the multiferroic properties of as-prepared $BiMn_{0.2}Fe_{0.8}O_3$ are greatly affected by the sintering temperature due to change in crystal structure and grain size.

Keywords: *$BiFeO_3$; structural transformation; sintering temperature; ferroelectric properties; magnetic properties.*

Introduction

The scientific community distinguishes between proper and improper ferroelectric magnetic perovskites referring to two different classes in which the ferroelectricity has an independent or a magnetostrictive origin, respectively. In proper ferroelectrics, the magnetic and electric ordering temperatures are usually different, so that the magnetoelectric effect is essentially absent, while the improper ferroelectrics have higher magnetoelectric coefficients but often quite low polarization intensity and very low ordering temperature of the

multiferroic phase. The Bi-based double perovskites can simultaneously yield high ordering temperatures and a consistent overlap between the two order types, thanks to a deep structural modification induced by the ordering process itself.[1] Also, there is an increasing interest of developing lead-free materials from the viewpoint of environmental protection.[2] In multiferroic materials, magnetism and ferroelectricity coexist, and if they are coupled they give rise to magnetoelectricity (ME) (or ferroelectromagnetism). Since most ferromagnets are conductive (with partially filled *d* -bands) and ferroelectrics are insulating (with filled bands), ferromagnetic ferroelectrics are scarce and currently non-existent at room temperature [3].

Among single-phase multiferroic materials, $BiMnO_3$ (BMO) and $BiFeO_3$ (BFO) have been extensively investigated. BMO is a rare multiferroic material which is FM (saturation moment, *M*S, of 3.6 μB /f.u). While the FE transition temperature is relatively high at 400 K, the FM transition temperature (T_C) is far below RT (T_C ~105 K), and the polarization is small (0.1 μC/cm^2 at ~90K).[4] BMO shows a weak negative magnetodielectric effect (MDE) near *T* C and exhibits a large gap between the FE and FM transition temperature.[5] To achieve practical ME applications of BMO, La-substitution on the *A* -site has been studied.[6] However, despite the enhancement of the ME effect, the *T*C remains low and the piezoresponse amplitude (d_{33}) of 2 pm/V is lower than BFO films (60 pm/V).[6,7]

In order to improve the electrical properties while preserving the magnetic ordering, several research groups adopted the strategy of doping $BiFeO_3$ with different +3 valence ions on A, B or both A and B sites [8–12]. The doping has resulted in the reduction of the leakage current density and in the improvement of the ferroelectric properties to some extent. Such substitutions were also expected to shift the transition temperature towards the room temperature. The Mn^{3+} (ionic radius = 0.645 Å) ions can occupy the Fe^{3+} sites in $BiFeO_3$ materials, because both ions have the same valence state and similar ionic size to that of Fe^{3+} (0.645 Å). Mn has one 3d electron less compared to Fe, which performs a perfect perturbation on the FeO_6 local structure [13]. Even if there are different oxidation states of Mn (3+, 4+) in Mn-doped $BiFeO_3$ materials, the ionic radii of the different oxidation states of Mn are comparable to that of Fe^{3+}. Consequently, the Mn ions can occupy the Fe sites only. Thus the present work focus on the effect of Mn substitution in BiFeO3 and its impact on the multiferroic properties.

Methodology

$BiMn_{0.2}Fe_{0.8}O$ has been synthesized by sol-gel auto-combustion technique. In order to prepare the $BiMn_{0.2}Fe_{0.8}O$ by sol-gel method, pure (>99.5%) AR grade corresponding metal nitrates were used. Citric acid solution was thoroughly mixed with the solution of metal nitrates under continuous stirring. Ammonia solution was slowly added in mixture to keep the pH at 7.0. The solution was continuously heated on magnetic hot plate at 90°C to evaporate the water content. With this, the solution became viscous and finally formed a gel. Upon continuous heating and stirring the gel was ignited and the combustion propagated forward until the entire gel burnt out to form porous $BiMn_{0.2}Fe_{0.8}O$ samples.

The prepared samples were characterizes by X-ray diffraction technique, X-ray diffraction patterns were recorded at room temperature in the 2θ range 20° to 70° using Cu-k_α radiation (λ=1.5404 Å). The magnetic properties such as saturation magnetization, magneton number, coercivity, remanence ratio etc. were studied by using Quantum Design Physical Property Measurement System. All the hysteresis curves were taken at room temperature. Ferroelectric properties of the samples were obtained by using an automatic P–E hysteresis loop tracer system. Dielectric properties with applied frequency were measured using LCR-Q meter.

Results and Discussion

X-ray diffraction (XRD) patterns of all the samples were obtained and studied for the crystal structure and to investigate the various structure phases resided in the as-prepared samples sintered at different temperature. The XRD patterns of the prepared samples sintered at different temperatures are shown in Fig. 1(a)-(c). It is evident that the sample sintered at 700 °C leads to a very poor crystallinity, whereas much better crystallized powders are obtained for ≥ 830 °C. It can be observed from Fig.1 that all the detectable diffraction peaks for the $BiMn_{0.2}Fe_{0.8}O_3$ nanoparticles matched to the distorted rhombohedral R3c structure. All the major XRD peaks may be indexed to the rhombohedral structure of $BiFeO_3$. Impurity phases are also observed for the samples sintered at 830 °C which are marked in the XRD patterns. It has been reported that the substitution of Mn brought about an orthorhombic crystal phase [space group P4mm and P4/mbm] and a suppression of secondary phases, where a mix phase of tetragonal and rhombohedral also obtained [14].

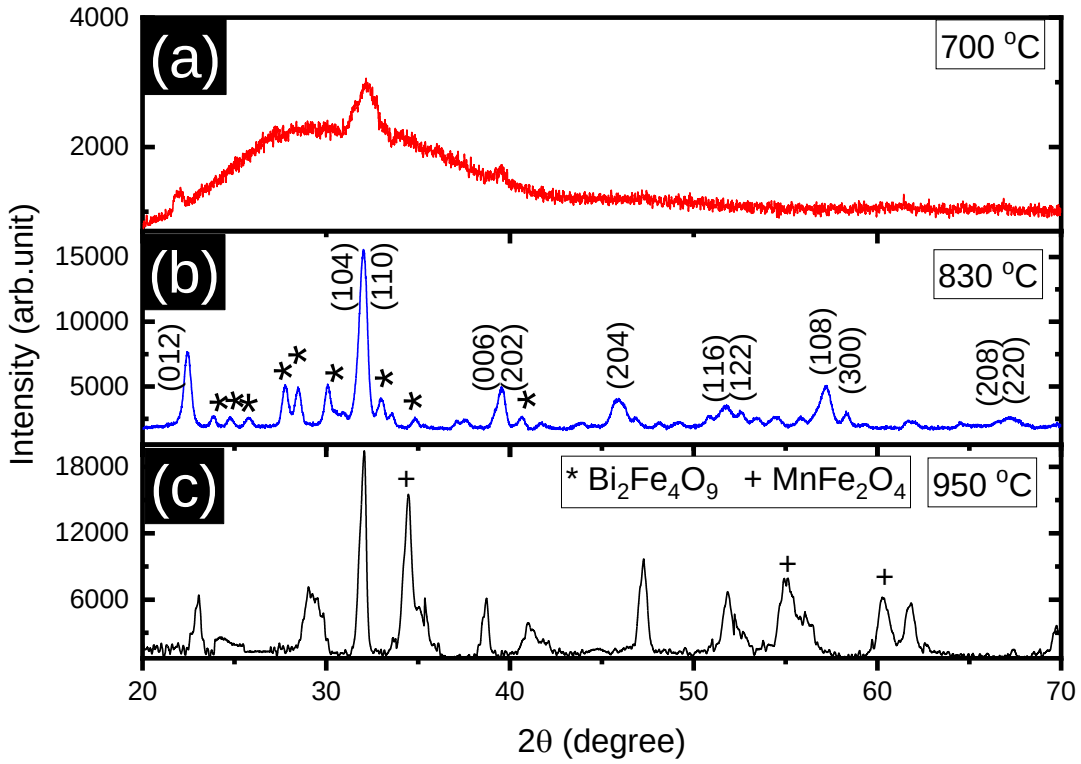

Fig. 1: X-ray diffraction patterns of $BiMn_{0.2}Fe_{0.8}O_3$ sintered at different temperatures. Asterisk (*) denotes the impurity phases whereas plus (+) denotes $MnFe_2O_4$ phase.

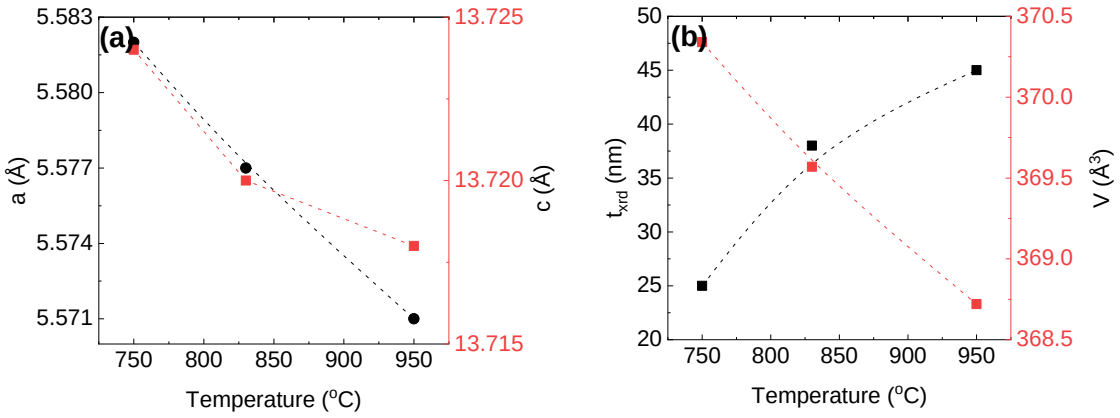

Fig. 2: (a) variation in lattice constant (a and c) with temperature, (b) variation in crystallite size (t_{xrd}) and unit volume cell with temperature.

The decrease in the lattice constant at higher sintering temperature is generally ascribed to the interface structure with a small volume fraction [15]. The increment role of the surface is easily detectable in the variation of lattice constant, which is becoming more important as the crystallite size varied.

Debye Scherrer [16] formula was used to calculate the crystallite size where the most intense peak (110) 2θ ≈ 31° was used:

$$t_{xrd} = \frac{k\lambda}{\beta cos\theta} \quad (1)$$

where β is full width at half maxima and k is the wavelength of Cu-Ka radiation which is 1.54 Å in the present case.

Variation in the crystallite size with sintering temperature can be viewed from Fig. 2b. Linear increase in crystallite size is observed with the increase in sintering temperature. While annealing decrease the strains and lattice defects, at the same time it may also cause coalescence of crystallites resulting in increase in the average crystallite size of the $BiMn_{0.2}Fe_{0.8}O_3$ nanoparticles [17].

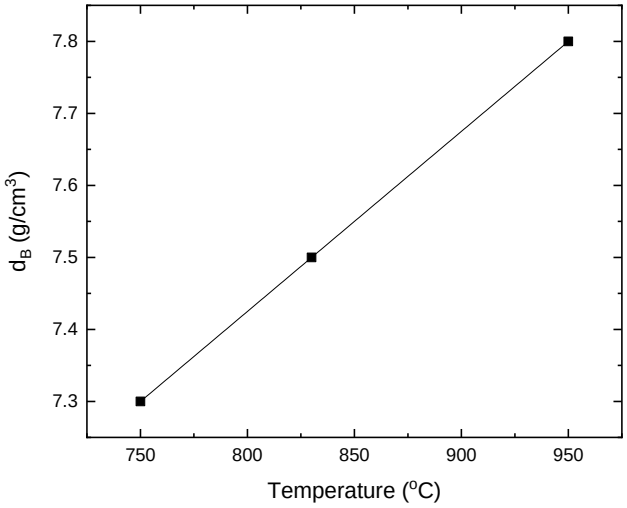

Fig. 3: (a) variation in bulk density (d_B) of all the samples of $BiMn_{0.2}Fe_{0.8}O_3$ nanoparticles measured at different temperature

Archimedes's method [18] was used to obtain the bulk density (d_B) of the samples:

$$d_B = \left[\frac{W_a}{W_a - W_W}\right]\frac{g}{cc} \quad (2)$$

where W_a and W_W are the weight of sample in air and water respectively. The variation of bulk density of the samples is shown in Fig. 3. The measured bulk densities are 7.3, 7.5 and 7.8 g/cm^3 for the samples sintered at 700, 830 and 950 °C respectively. The densities of the samples sintered at lower temperature are lower than those obtained at higher sintering temperature. The higher sintering temperature treatment resulted in the increase in crystallite

size and reduced the pore fraction leading to densify the samples. Eventually the porosity of the samples decreased at higher sintering temperature.

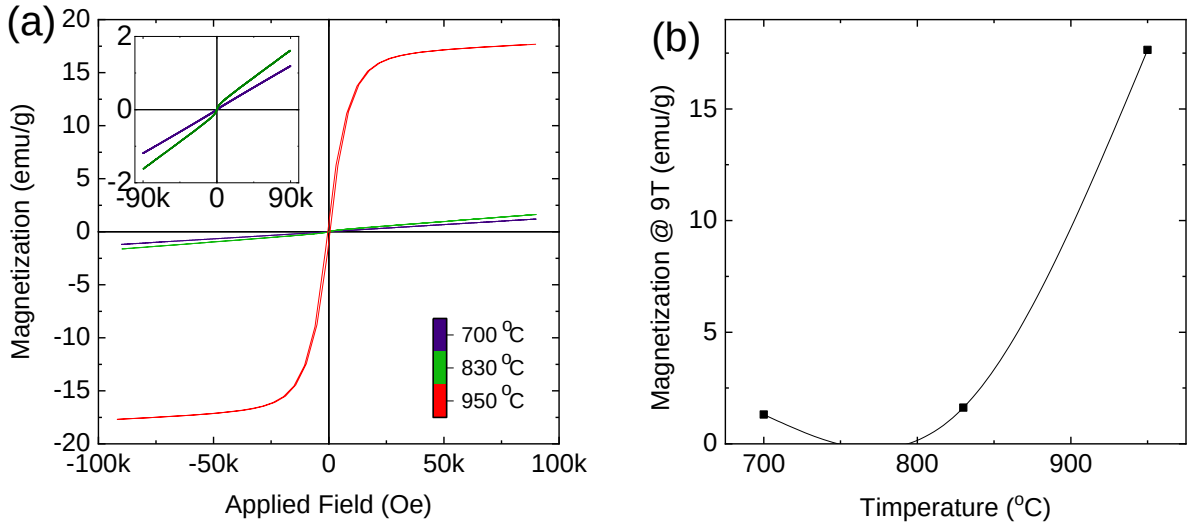

Fig. 4: (a) Variation in magnetization (H) with applied magnetic field (M), (b) variation of magnetization at 9T for all the samples of $BiMn_{0.2}Fe_{0.8}O_3$ measured at different temperature. Inset of panel 'a' shows M-H curves of samples sintered at 700 and 830 °C.

Magnetic properties of all the prepared samples were studied at room temperature. The variation in magnetization (M) with applied magnetic field (H) (magnetic hysteresis loop or M–H loops) of $BiMn_{0.2}Fe_{0.8}O_3$ nanoparticles sintered at 700, 830 and 900 °C are shown in Fig. 4. $BiMn_{0.2}Fe_{0.8}O_3$ sintered at 700 °C do not shows a linear hysteresis loop which is a typical antiferromagnetic behaviour with almost negligible zero coercivity and zero remanent magnetization. Sample sintered at 830 °C show improvement in magnetic characteristic where ferro/ferromagnetic nature of prepared sample is observed, although the magnetization curves are not yet saturated with at applied magnetic field of 9T. However, the largest saturation magnetization is observed for the sample sintered at 900 °C. Increase in magnetization with temperature may be related to the following facts [19]: (i) the increase in spin canting (Jahn-Teller distortion) due to the modification in Fe–O–Fe bond angle resulted in the net macroscopic magnetization [20-22]; (ii) The increase in crystallite size with increase in sintering temperature; and (iii) the structural phase transition, first to rhombohedral to other phases occurred with increase in sintering temperature. Such changes in the structural properties may destroys the spin cycloid resulting in releases of locked magnetization. In particular the largest value of Ms observed in the sample sintered at 900 °C is mainly attributed to the ferromagnetic $MnFe_2O_4$ cubic spinel ferrite phase formation. In

general, the increase in sintering temperature resulted in increase in saturation magnetization, where higher magnetization is associated with higher crystallite size. The increase in saturation magnetization at larger particles is ascribed to the reactive surface layer that has higher magnetization. In other words, smaller particles have dead-surface (non-reactive) layer which has smaller magnetization. Thus, in the presence of such dead surface layer, the magnetization of the particles do not attain the saturation with the increase in applied magnetic field. The core magnetic moments align with the applied magnetic field up to a certain applied magnetic field. The magnetization response of the 'core mode' can be exhausted after a certain value of applied magnetic field and thus the 'core magnetization' of the material is saturated in a Langavin-like way. After this point the increase in the applied magnetic field has an effect only on the surface layer of the particles resulting in the gradual slow-down in the increase in magnetization [23]. Absence of magnetic saturation with a very low coercivity value was observed at such a specific stage of the core shell morphology of nanoparticles [24]. The small magnetization value of magnetization for small particle size are difficult to justify by only considering surface effects. Some alternative reason for smaller value of magnetization at smaller particles are; (i) Yafet-Kittle type spin canting may be present in the whole volume of the particle; (ii) variation in site occupancy of ions with the sintering temperature, (iii) disordered surface layer and (iv) change in crystal structure with temperature [25, 26]. Therefore, in addition to the surface effect, the order–disorder characteristic of the samples also has a strong effect on the magnetic properties of the prepared samples.

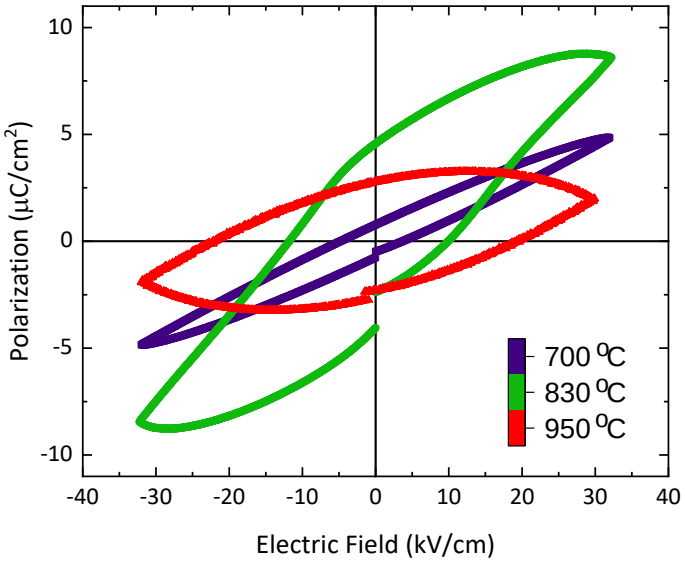

Fig. 5: Variation in polarization (P) with applied electric field (E) for all the samples of $BiMn_{0.2}Fe_{0.8}O_3$ measured at different temperature.

Polarization with electric field (P-E) hysteresis loops of all the $BiMn_{0.2}Fe_{0.8}O_3$ samples sintered at different temperatures are shown in Fig. 5. P-E hysteresis loop for the sample sintered at 700 °C are not saturated and shows a remanent polarization (Pr) of 0.83 $\mu C/cm^2$ which increased to 4.54 $\mu C/cm^2$ for the sample sintered at 830 °C. These P-E loops show that the polarization value of $BiMn_{0.2}Fe_{0.8}O_3$ increased with the increase in sintering temperature, which is true for the samples sintered at 700 and 830 °C. However, decrease in Pr observed when samples sintered at 950 °C. The modified ferroelectricity/polarization may be ascribed to the structural distortion, increased grain size, high density, low porosity and absence of unavailability of centers for the pinning effect. grain size affect the domain nucleation, domain structure and domain mobility which affect the ferroelectric properties of ferroelectrics materials [27]. With the increasing grain size, domains in the ferroelectric nanoparticles become easier to be switched with the applied electric field. At the same time, grain size can affect the number of the defects where larger grain size reduced the defects. Thus, the sample sintered at 700 °C with lowest crystallite size among all the samples experiences more depression of ferroelectric characteristics. The grain boundaries behave as a pinning centre for polarization that interrupt the polarization switching. Enhanced polarization may also arise from the distorted symmetry with the contribution of dipolar defect complexes. Further, the smaller grain size generally forms higher number of grain boundaries. High internal stresses usually produce around the grain boundaries and especially at their triple-point junctions. This gives the growth of minor domains at the grain boundaries and at their junctions which is beneficial in the improvement in the ferroelectric properties [28]. In the present scenario, grain size affect the ferroelectric properties, however the crystal structural characteristics plays a vital role in modifying the ferroelectric properties.

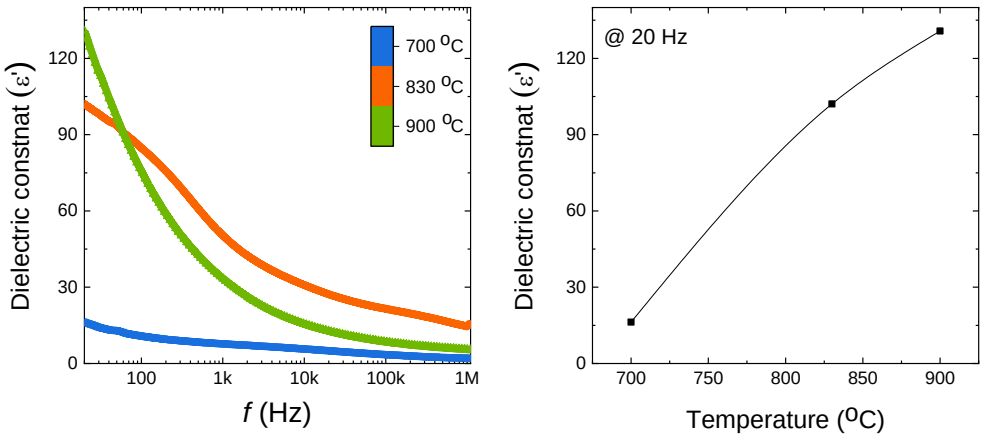

Fig. 6: Variation in real part of dielectric constant (ε') with frequency for all the samples of $BiMn_{0.2}Fe_{0.8}O_3$ measured at different temperature.

Fig. 6 exhibit the dielectric constant of $BiMn_{0.2}Fe_{0.8}O_3$ nanoparticles measured as a function of frequency. The measurements were done at room temperature in the frequency range of 20 Hz to 1 MHz. Figure 5 shows that the dielectric constant of all the $BiMn_{0.2}Fe_{0.8}O_3$ samples decreased with increase in frequency. Such a decrease in dielectric constant is ascribed to the inertia possessed by charges that hinder the spontaneous polarization switching with the application of electric field. At lower frequency, dielectric constant decreased rapidly because of the charge accumulation effect. Such a spontaneous polarization dispersion at the lower frequency level is a common characteristics of ferroelectrics ascribed to the small ionic conductivity [29]. As more dielectric dispersion is observed at low frequency region for the sample sintered at 950 °C, this observed behaviour may be due to the Maxwell-Wagner interfacial type of polarization [30, 31], which is in agreement with Koops phenomenological theory [32]. Ferrite phase of $MnFe_2O_4$ is observed for the sample 950 °C whose dielectric structure was supposed to be made of two layers, insulating grain boundary and grain of high conductivity. The motion of charges in grains is interrupted at the grain boundaries under the application of applied electric field that causing accumulation of localized charge at the interface that resulted in interfacial polarization. The linear decrease of dielectric constant with increase in frequency is due to the fact that beyond a certain frequency of the electric field, the electronic exchange among Fe^{3+} and Fe^{2+} does not follow the alternating field. Increase in sintering temperature increase the dielectric constant of the system as observed from Fig. 6. Such behaviour of dielectric constant is relative to the variation in grain size, density and porosity of the materials. Porosity is higher at lower sintering temperature that reduce the space charge build-up resulted in lower value of polarization/dielectric constant at lower sintering temperature. Vice-versa electron motion are easier in bigger grains that has more contact among the adjacent grains, which enables easy flow of electrons towards the grain boundaries. Increase in formation of Fe^{2+} from Fe^{3+} at higher sintering temperature may also results to increase in the dielectric constant with increase in sintering temperature [33].

Conclusions

$BiMn_{0.2}Fe_{0.8}O_3$ samples were synthesized by a chemical route called sol–gel auto-combustion method. The as synthesized $BiMn_{0.2}Fe_{0.8}O_3$ powder was sintered at three different temperatures viz. 700, 830 and 950 °C. XRD patterns shows that the sample sintered at 700 °C is amorphous where sample crystallized in rhombohedral phases while sintered at

830 °C. Further, increase in sintering temperature to 950 °C transformed the material into mix phase, where $MnFe_2O_4$ is one of the major phases observed. Crystallite and grain size increased with the increase in sintering temperature. Such a change in the crystal structure and grain size greatly affects the multiferroic properties of $BiMn_{0.2}Fe_{0.8}O_3$. Maximum polarization is observed in case of sample sintered at 830 °C, whereas maximum magnetization and dielectric constant observed for the sample sintered at 950 °C. Among all the studied materials; the sample sintered at 850 °C shows the best multiferroic properties, which is related to the crystal structure and increased grain size.

References

[1] D. Delmonte, F. Mezzadri, E. Gilioli, M. Solzi, G. Calestani, F. Bolzoni, R. Cabassi, Inorg. Chem. 2016, 55, 6308−6314

[2] S. E. Shirsath, C. Cazorla, T. Lu, L. Zhang, Y. Y. Tay, X. Lou, Y. Liu, S. Li, D. Wang, Nano Letters 20 (2020) 1262-1271

[3] N. A. Hill, J. Phys. Chem. B 2000, 104, 6694.

[4] A. M. Dos Santos, S. Parashar, A. R. Raju, Y. S. Zhao, A. K. Cheetham, C. N. R. Rao, Solid State Commun. 2002, 122, 49.

[5] T. Kimura, S. Kawamoto, I. Yamada, M. Azuma, M. Takano, Y. Tokura, Phys. Rev. B. 2003, 67, 180401(R).

[6] M. Gajek, M. Bibes, S. Fusil, K. Bouzehouane, J. Fontcuberta, A. Barthélémy, A. Fert, Nat. Mater. 2007, 6, 296.

[7] S. Y. Yang, F. Zavaliche, L. Mohaddes-Ardabili, V. Vaithyanathan, D. G. Schlom, Y. J. Lee, Y. H. Chu, M. P. Cruz, Q. Zhan, T. Zhao, R. Ramesh, Appl. Phys. Lett. 2005, 87, 102903.

[8] Y.K. Jun, W.T. Moon, C.M. Chang, H.S. Kim, H.S. Ryu, J.W. Kim, K.H. Kim, H.S. Hong, Solid State Commun. 135 (2005) 133–137.

[9] S.K. Singh, H. Ishiwara, K. Maruyama, Appl. Phys. Lett. 88 (2006) 262908.

[10] C.F. Chung, J.-P. Lin, J.-M.Wu, Appl. Phys. Lett. 88 (2006) 242909.

[11] X. Qi, J. Dho, R. Tomov, M.G. Blamire, J.L. MacManus-Driscoll, Appl. Phys. Lett. 86 (2005) 62903.

[12] J.K. Kim, S.S. Kim, W.J. Kim, Appl. Phys. Lett. 88 (2006) 132901.

[13] R.D. Shannon, Acta Crystallogr., Sect. A: Cryst. Phys., Diffr., Theor. Gen. Crystallogr. 32 (1976) 751.

[14] Y. Han, Y. Ma, C. Quan, N. Gao, Q. Zhang, W. Mao, J. Zhang, J. Yang, X. Li, W. Huang, Ceram. Inter. 41 (2015) 2476–2483.

[15] Gleiter, H. Prog. Mater. Sci. 1989, 33, 223.

[16] S. E. Shirsath, S. S. Jadhav, B. G. Toksha, S. M. Patange, K. M. Jadhav, J. Appl. Phys. 110, 013914 (2011)

[17] Raming, T. P.; Winnubst, A. J. A.; van Kats, C. M.; Philipse, A. P. J. Coll. Inter. Sci. 2002, 249, 346-350.

[18] S. E. Shirsath, B.G. Toksha, K.M. Jadhav, Mater. Chem. Phys. 117 (2009) 163–168

[19] V.R. Palkar, D.C. Kundaliya, S.K. Malik, J. Appl. Phys. 93 (2003) 4337.

[20] S.K. Srivastav, N.S. Gajbhiye, A. Banerjee, J. Appl. Phys. 113 (2013) 203917.

[21] C. Ederer, N.A. Spaldin, Phys. Rev. B 71 (2005) 060401.

[22] J. Weia, D.S. Xue, Appl. Surf. Sci. 258 (2011) 1373.

[23] Hasmonay, E.; Depeyrot, J.; Sousa, M.H.; Tourinho, F.A.; Bacri, J.C.; Perzynski, R.; Raikher, Y. L.; Rosenman, I. J. Appl. Phys. 2000, 88, 6628-6635.

[24] Caizer, C.; Stefanescu, M. J. Phys. D 2002, 35, 3035-3040.

[25] Vollath, D.; Szabo, D.V.; Taylor, R.D.; Willis, J.O. J. Mater. Res. 1997, 12, 2175–2182.

[26] Martinez, B.; Obradors, X.; Balcells, L.L.; Rouanet, A..; Monty, C. Phys. Rev. Lett. 1998, 80, 181-184.

[27] C.C. Leu, C.Y. Chen, C.H. Chien, M.–N. Chang, F.–Y. Hsu, C.–T. Hu, Appl. Phys. Lett. 82 (2003) 3493.

[28] H. Hu, S.B. Krupanidhi, J. Mater. Res 9 (1994) 1484–1498.

[29] N. Choudhary, D.K. Kharat, D. Kaur, Surf. Coat. Technol. 205 (2011) 3387–3396.

[30] Maxwell, J. C. Electricity and Magnetism, Oxford University Press, Oxford. Section 328, 1,

[31] Wagner, K. W. Ann. Phys. (Leipzig) 1913, 40, 817.

[32] Koops, C. G. Phys. Rev. 1951, 83, 121.

[33] Jahanbin, T.; Hashim, M.; Mantori, K. A. J. Magn. Magn. Mater. 2010, 322, 2684-2689.